Chapter 9
Parametric Studies on Prediction of Temperature and Restrained Strain of Mass Concrete

9.1. General

The use of the proposed computerized model is beneficial for selecting mix proportion and design proper construction process for mass concrete. The suitable use of mix proportion such as fly ash replacement ratio, type of fly ash, and type of aggregate can prevent thermal cracking. The use of different type of aggregate has an effect on thermal properties of concrete which influences semi-adiabatic temperature, thermal stress and restrained strain. The proposed model is used to help engineer to design proper construction processes such as casting method and curing condition. In the case of massive concrete with very large size, casting usually can not be finished at one time. Technique of discontinuous casting typically layer casting or block casting was used in order to minimize temperature gradient of mass concrete. The selection of proper dimension and numbers of concrete blocks or layers in order to prevent thermal cracking is one of the important steps of the mass concrete construction. The curing method and curing period are also important to prevent thermal cracking during the construction process. Many massive structures crack because of the application of unsuitable curing method and curing period. The objective of this study is to explain and propose a method to compute the temperature and restrained strain in mass concrete by taking into account the footing dimension, casting method, aggregate type, curing condition and curing period in order to prevent thermal cracking.

In the analysis, *h* (convection heat loss) at the top surface are assumed to be equal to 4 and 10.6 kcal/m^2 hr ^{o}C for insulation (IC) and normal curing (NC), respectively. The difference of these two types of curing is on the material which is used to cover the top surface. In the case of NC, the top surface was not insulated while for insulated curing, the top surface was covered by foam. By the use of the insulation material, the surface heat loss at the top surface was controlled then *h* of NC is higher than that of insulation curing. The *h* at bottom and side surfaces are assumed to be equal to 2.5 kcal/m^2 hr ^{o}C . The average annual temperature of Bangkok which is equal to 28.7 ^{o}C (Jindawanik et al., 2000) is used as the atmospheric boundary condition. The initial condition of concrete is the initial temperature of concrete which is assumed to be 30 ^{o}C.

From the example of the analytical results in Chapter 8, in case of temperature, point A shows the lowest but point B shows the highest temperature. For illustration in this chapter, points A and B are used to describe the lowest and highest temperature. The restrained strain in tension at point A is the highest then the results at point A are used to describe the maximum restrained strain in tension ($\varepsilon_{res,\ ten}$) in this chapter. The maximum restrained strain in tension ($\varepsilon_{res,\ ten}$) of footing obtained from the proposed model is compared with the other researchers's results of tensile strain capacity (TSC) of concrete and if $\varepsilon_{res,\ ten}$ is higher than TSC then the mass concrete structure is evaluated to crack.

9.2. Analytical Parameters

The mix proportion and properties of concrete used in the analysis are shown in Table 9.1. Mix 1 was used to study the effect of dimension (especially thickness), construction method and curing condition of mass concrete structure. Mix 2 was used to investigate the effect of casting period. Mixes 1 and 3 were used to investigate the effect of type of aggregate and mix 1 and 4 were for the effect of fly ash content.

9.2.1 Effect of mix proportion

a) Type of aggregate
Limestone and Quartz were used as coarse aggregates for mixes 1 and 3 in Table 9.1, respectively. The dimensions of 33 x 49.2 x 2.5 m. and insulation curing were used in the analysis.

b) Type of fly ash
Footing with dimensions of 33 x 49.2 x 2.5 m. was used in the analysis. Two types of fly ash (FA1 and FA2) were compared in this study. Both of them are assumed to have the same physical properties but the chemical compositions are different. The CaO content of FA2 is lower than FA1. The physical properties and chemical compositions of fly ash shown in Table D6 and D7 were used in this illustration. Mix 1 in Table 9.1 was used in the analysis.

c) Percentage of fly ash replacement
Footing with dimension of 33 x 49.2 x 2.5 m. was used in the analysis. Mixes 1 and 4 in Table 9.1 were used in the analysis and both mixes were designed to have equal compressive strength at 56 days.

Table 9.1 Mix proportion and properties of concrete and ingredients

Mix No.	1	2	3	4
Cement (kg/m^3)	212	242	212	269
Fly Ash (kg/m^3)	212	198	212	145
Water (kg/m^3)	166	185	166	180
Coarse Aggregate (kg/m^3)	1120	1000	1120	1120
Fine Aggregate (kg/m^3)	700	780	700	700
Type of Coarse Aggregate	Limestone	Limestone	Quartzite	Limestone
E at 28 days (MPa)	28000	27000	28000	28000
ν	0.2	0.2	0.2	0.2

Remark: E and ν are modulus of elasticity and poisson ratio.

9.2.2 Effect of dimension

a) Thickness of structure

In order to investigate the effect of thickness of mass concrete, the thickness was varied to be 0.5, 1.0, 1.5, 2.0, 2.5, 3.0, 4.0, 5.0, 6.0, 8.0 and 10.0 m. whereas the width and length were fixed at 33 and 49.2 m., respectively. An example of description of the dimension designation is as follow; "d0.5" means the structure which has sizes of 33 x 49.2 x 0.5 m. Insulation curing was used in the analysis.

b) The ratio of the exposed surface area to volume of concrete (S/V)

The dimensions of the concrete used in the analysis were shown in Table 9.2. The volume and thickness of the concrete were fixed at 4059 m^3 and 2.5 m., respectively. The exposed surface area (S) is defined as the summation of the area of all surfaces except the bottom surface of concrete. The insulation curing was used in the analysis.

9.2.3 Effect of construction method

a) Casting Period

A structure with dimensions of 38.4 x 8.4 x 4.76 m. using concrete mix no. 3 as shown in Table 9.1 was used to investigate the effect of continuous casting period. The analysis is divided into two cases which are casting with and without consideration of casting period. For the case without consideration of casting period (CC), the concrete block was assumed to be cast and completed within a very short period or the casting of bottom part was assumed to be completed at the same time as that of the top part. In case of the analysis with consideration of casting period (LC), the casting of bottom part of concrete block was assumed to be completed many hours before the completion of the top part. According to the large size of mass concrete, the casting period of a footing is usually very long. The reaction of the previously cast concrete has already started many hours before the last batch of concrete is cast. Therefore, it is important to investigate the effect of casting period in the analysis. The casting period in the analysis was assumed to be 24 hours.

b) Casting Methods

Two types of casting methods i.e. continuous casting and discontinuous casting were used in the analysis. In case of discontinuous casting method, the mass concrete was divided and cast in many small sizes. Temperature gradient of mass concrete was minimized by using the technique of layer casting or block casting. In this study, various cases of discontinuous casting were used in the analysis as shown in Fig 9.1. The dimensions of casting block or layer are shown in Table 9.3. Mass concrete was assumed to be cast in 2 parts for both layer casting and block casting (see numbers 1 and 2 in Figs 9.1a to 9.1d). The second part was cast 2 weeks after the completion of the first part. The volume of concrete for each part was fixed at 2435.4 m^3. Insulation curing was applied to the top surface for all cases. In order to simulate the most critical situation that occur at the joints of block casting, the boundary condition at the joint of the first part is modeled to be steel formwork to let the heat at the joints of the first casting of the block evacuate faster. From previous study (Kwak et al., 2006), the convective heat transfer coefficient for steel formwork is equal to 7.5 kcal/m^2 hr ^oC. This value was used in this analysis.

Table 9.2 Dimensions of Mass Concrete

No.	W (m.)	L (m.)	T (m.)	V (m^3)	S (m^2)	S/V (m^{-1})
d25	33.0	49.2	2.5	4059	2035	0.501
vs1	40.295	40.295	2.5	4059	2027	0.499
vs2	6.5	249.8	2.5	4059	2905	0.716
vs3	3.5	463.9	2.5	4059	3961	0.976
vs4	2.5	649.5	2.5	4059	4884	1.203

Remark: W, L and T are width, length and thickness of concrete.

Table 9.3 Dimensions of layer and block in different casting methods

Casting method	Notation	Dimension of layer or block (m.)
Continuous casting	Con	33.0 x 49.2 x 3.0
Discontinuous casting : 2 Layers	2L	33.0 x 49.2 x 1.5
Discontinuous casting : 2 Blocks	2B	33.0 x 24.6 x 3.0
Discontinuous casting : 4 Blocks	4B	33.0 x 12.3 x 3.0

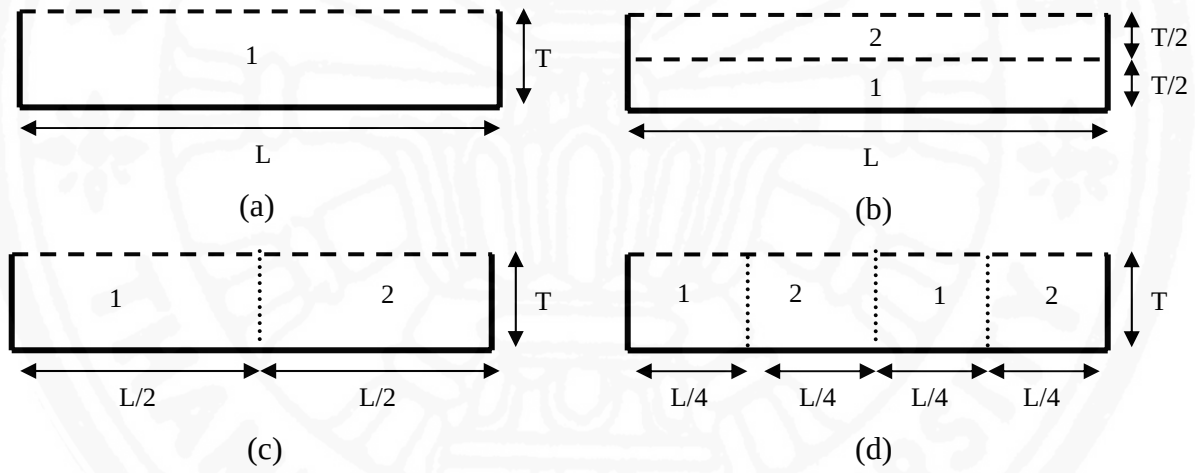

Remark : _ _ _ _ Insulated surface, _____ Subsoil, ... Steel formwork

Fig. 9.1 Casting step of mass concrete (side view). (a) Continuous casting. (b). Discontinuous casting with 2-layer casting. (c). Discontinuous casting with 2-block casting. (d) Discontinuous casting with 4-block casting.

c) Curing condition and curing period.

Structure with dimension of 33.0 x 49.2 x 2.5 m. was used to investigate the effect of curing condition and curing period. Two types of curing i.e. normal curing (NC) and insulation curing (IC) were analyzed. The difference of these two types of curing is on the material which is used to cover the top surface. In the case of NC, the top surface was not insulated while for insulation curing, the top surface was covered with foam. By the use of the insulation material, the surface heat loss at the top surface was controlled then *h* of NC is higher than that of the insulation curing. For insulation curing, the curing periods were divided into two cases i.e. continuous insulation curing (CIC) and discontinuous insulation curing (DIC). For continuous insulation curing (CIC), the insulation material was kept until

the end of the analysis while for the discontinuous insulation curing (DIC), the insulation materials was removed a few days after the peak temperature was reached.

9.3 Analytical Results

9.3.1 Effect of mix proportion.

a) Effect of type of aggregate

Figs. 9.2 and 9.3 show the comparison of temperature and $\varepsilon_{res,\ ten}$ of concrete with different types of coarse aggregate. As shown in Table 9.4, Quartzite and Limestone have nearly the same specific heat (*c*) but quartzite has higher thermal conductivity (*k*) than limestone. As a result, during heating up, the temperature of concrete made with these aggregates is nearly the same, however during the cooling down stage the temperature of quartzite concrete decreases faster than that of the limestone concrete (as shown in Fig. 9.2). The coefficient of thermal expansion (*CTE*) of quartzite is much higher than that of the limestone then the restrained strain of quartzite concrete is much higher than that of the limestone concrete and higher than TSC (see Fig. 9.3). In this case, the use of quartzite as coarse aggregate causes thermal crack. It can be concluded that for mass concrete limestone is generally more appropriate than quartzite due to much lower *CTE* which reduces restrained strain.

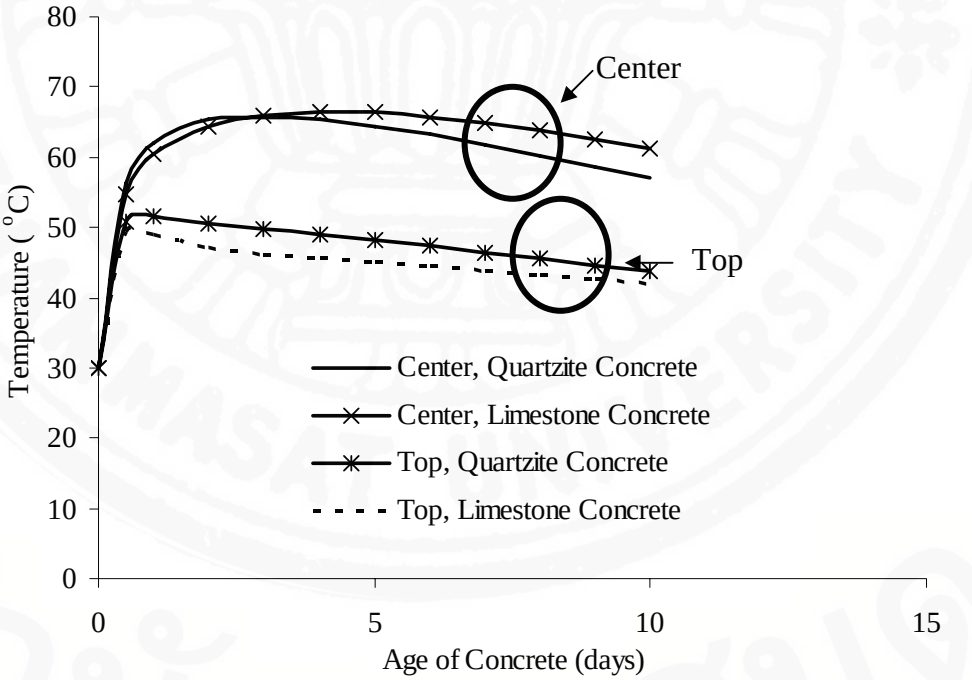

Fig. 9.2 Predicted temperature of mass concrete with limestone and quartzite as coarse aggregates

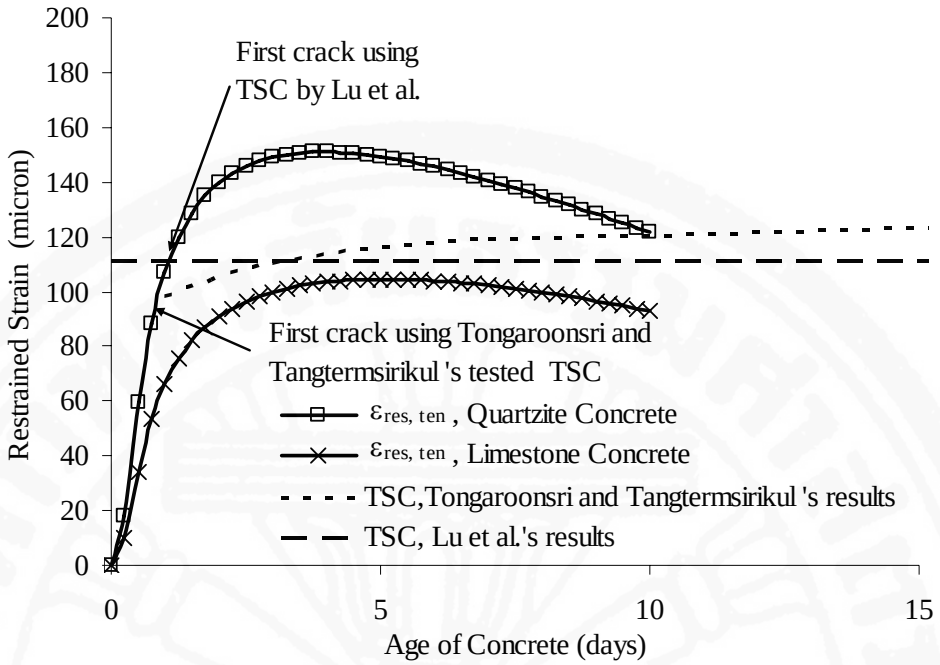

Fig. 9.3 Predicted restrained strain of mass concrete with limestone and quartzite as coarse aggregates

Table 9.4 Thermal Properties of Limestone and Quartzite

Type of Rock	Specific Heat, c, (kcal/kg ^{o}C)	Thermal Conductivity, k (kcal/m hr ^{o}C)	Coefficient of Thermal Expansion, CTE (micron/°C)
Limestone	0.20 (Klieger and Lamond, 1994)	2.20 (Klieger and Lamond, 1994)	4.5 (Klieger and Lamond, 1994)
Quartzite	0.18 (Klieger and Lamond, 1994)	3.10 (Klieger and Lamond, 1994)	12.5 (Klieger and Lamond, 1994)

b) Effect of type of fly ash

Figs 9.4 and 9.5 show the prediction of temperature and restrained strain of mass concrete with different types of fly ash. The use fly ash with higher CaO content increases temperature of mass concrete then the restrained strain is higher. It can be concluded from the analytical result that the use of fly ash with low CaO content is preferable for mass concrete.

c) Effect of the percentage of fly ash replacement

Fig. 9.6 and Fig. 9.7 show the prediction of temperature and restrained strain of mass concrete with different fly ash replacement ratios (r). It can be seen that temperature decreases with the increase of the amount of fly ash, as a result, the restrained strain becomes smaller. It is well known that the use of fly ash to partially replace cement reduces temperature of mass concrete and the proposed model also shows the consistent results. Both mixes were designed to have the same compressive strength however the use of mix with lower fly as replacement ratio results in thermal cracking. The selection of mix proportion for mass concrete based on only compressive strength is not appropriate for mass concrete structure. Engineer must also

concern and design concrete mix proportion to prevent thermal cracking by considering proper materials for mix proportioning.

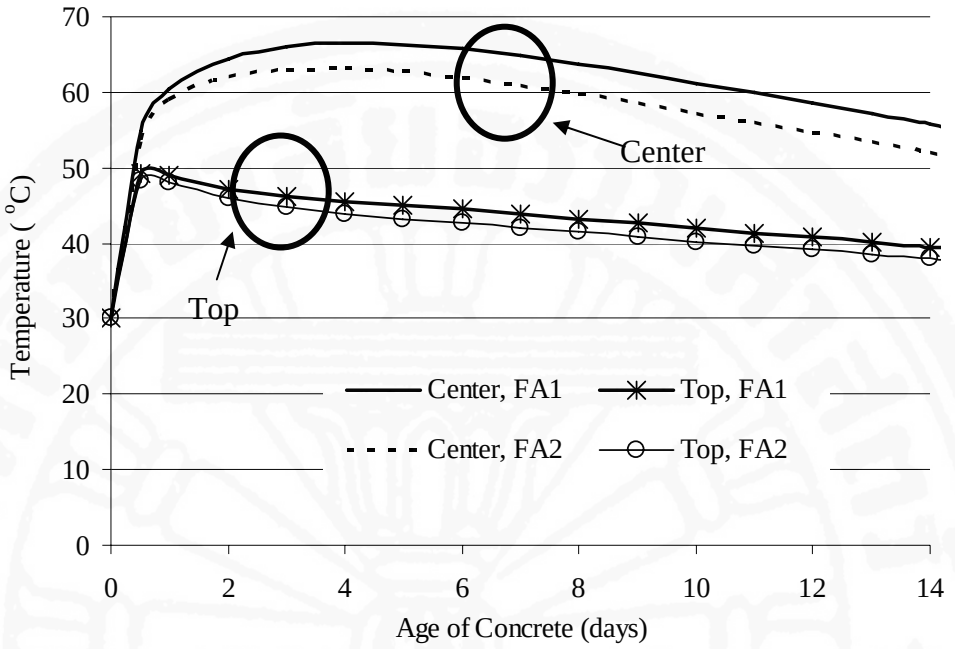

Fig. 9.4 Predicted temperature of mass concrete with different types of fly ash

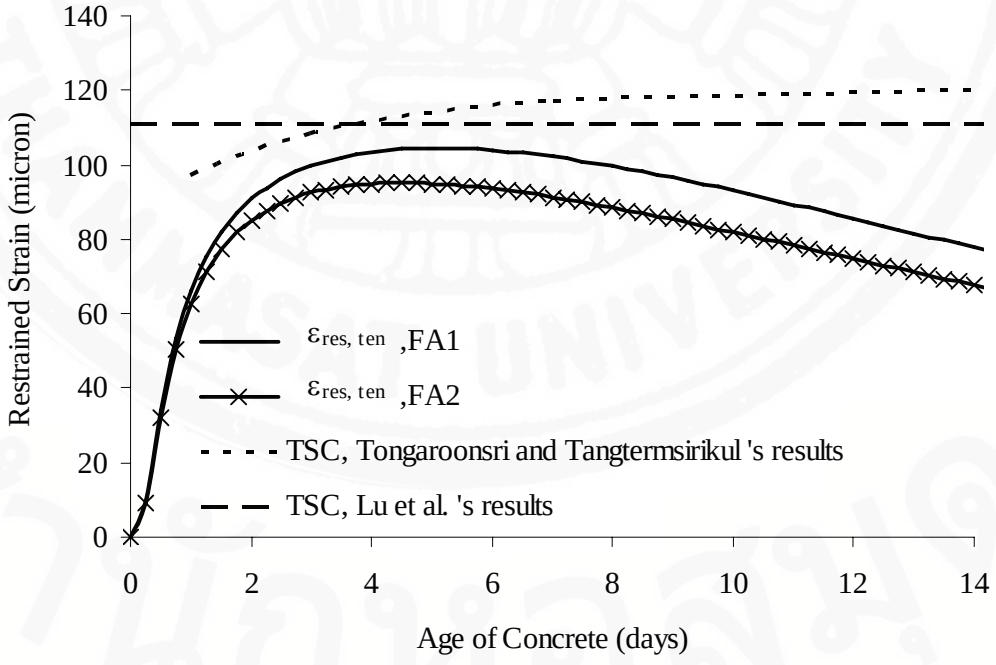

Fig. 9.5 Predicted restrained strain of mass concrete with different types of fly ash

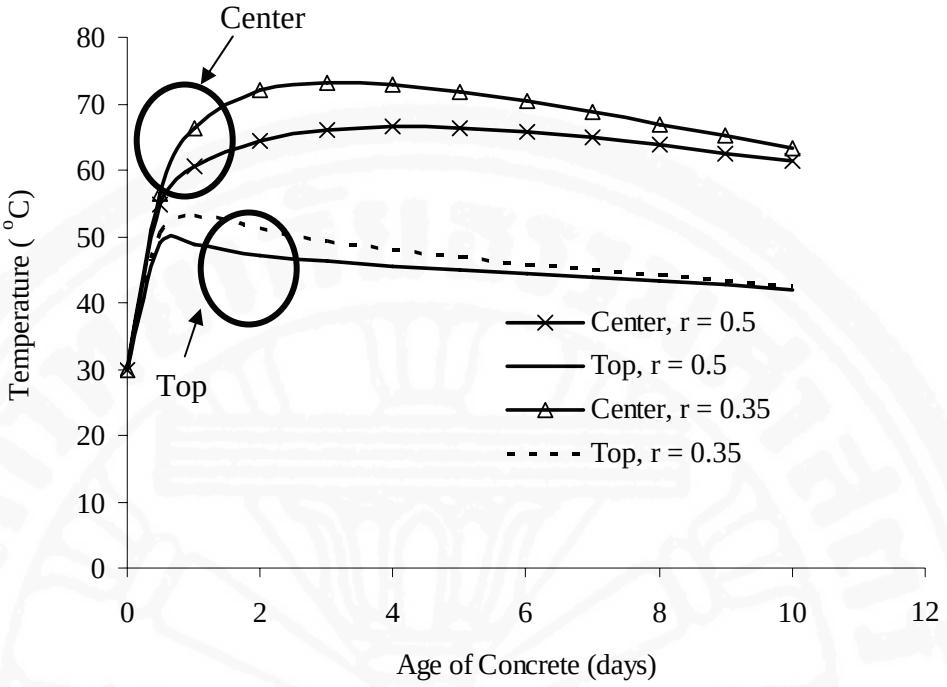

Fig. 9.6 Predicted temperature at center and top surface of mass concrete with fly ash replacement ratios of 0.35 and 0.5

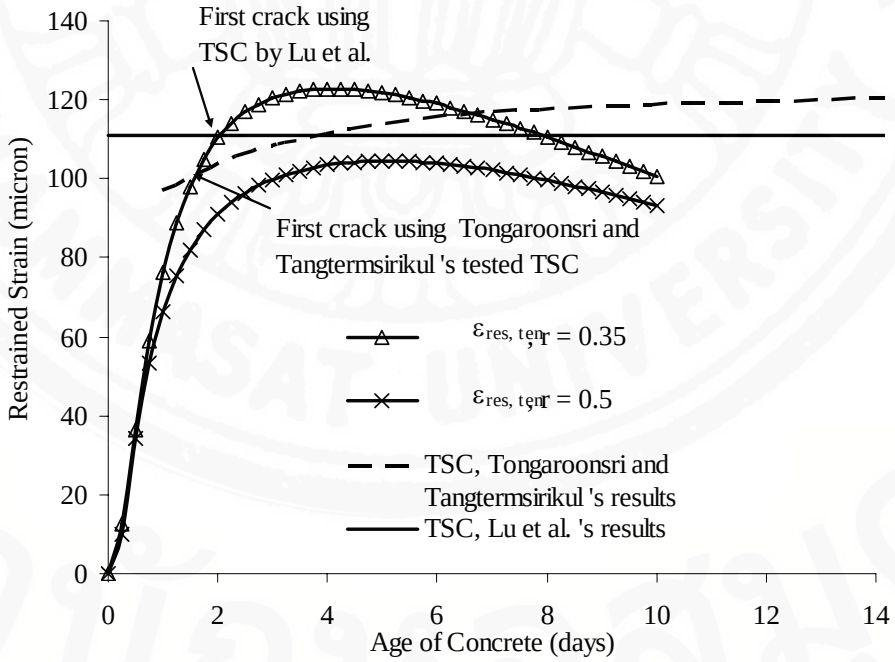

Fig. 9.7 Predicted restrained strain of mass concrete with fly ash replacement ratios of 0.35 and 0.5

9.3.2 Effect of dimension

a) Effect of thickness of structure

Fig. 9.8 shows the prediction of temperature at the center of mass concrete with different thickness. It can be seen that temperature increases with the increase of thickness of the mass concrete and the peak is gained at the longer age. Fig. 9.9 shows the relationship between the maximum temperature at the center and the thickness of the mass concrete. The maximum temperature increases with the increase of the thickness. However, when the thickness is higher, the rate of increase becomes smaller. When the thickness is large, the behavior of the mass concrete becomes nearly adiabatic. The $\varepsilon_{res,\ ten}$ (see Fig. 9.10) shows the same tendency as that of the temperature because temperature difference between center and surface is higher when the thickness increases.

b) Effect of the ratio of the exposed surface area to volume of concrete (S/V)

Fig. 9.11 shows the values of the maximum temperature at the center to S/V of mass concrete. The maximum temperature reduces with the increase of s/v. It can be concluded that the use of only volume or thickness of concrete may not be enough for estimating the maximum temperature. Exposed surface area is another preferable parameter.

9.3.3 Effect of construction method

a) Casting period

Figs. 912 to 9.14 show the comparison between test and predicted results at center, bottom and top parts of mass concrete, respectively. The model was satisfactory to predict temperature of mass concrete. It was found that the predictions of temperature for both CC and LC are nearly the same except during the first few hours (during casting and a few hours after casting). The analysis with consideration of casting period (LC) is more accurate when compared to the CC case especially during the first few hours. It can be concluded that, for very large mass concrete structure, the casting period must be considered in order to increase the accuracy of the temperature prediction especially during the concrete casting period.

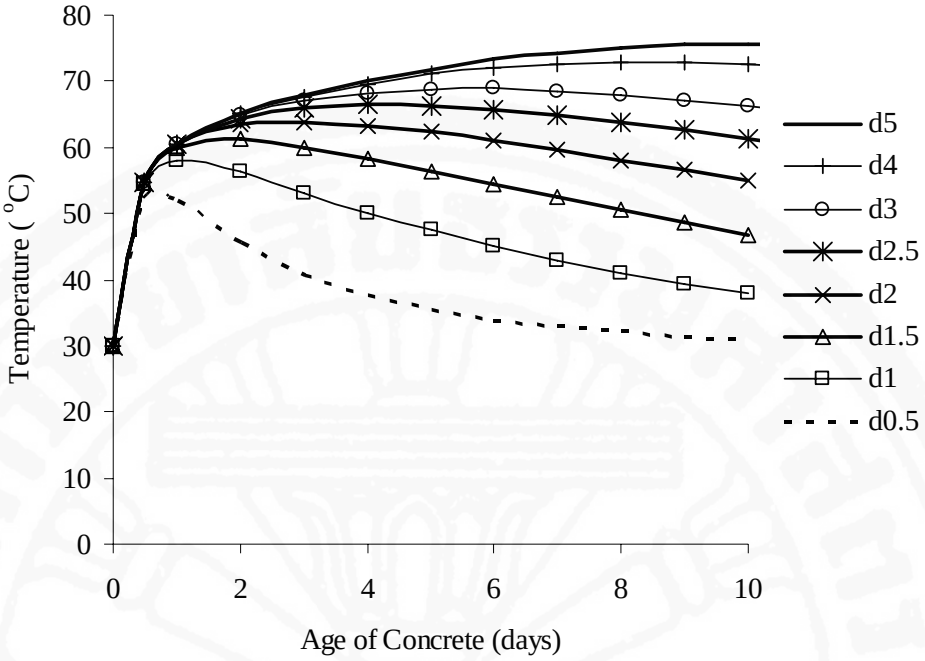

Fig. 9.8 Predicted temperature of mass concrete with different thickness (width = 33 m., length = 49.2 m)

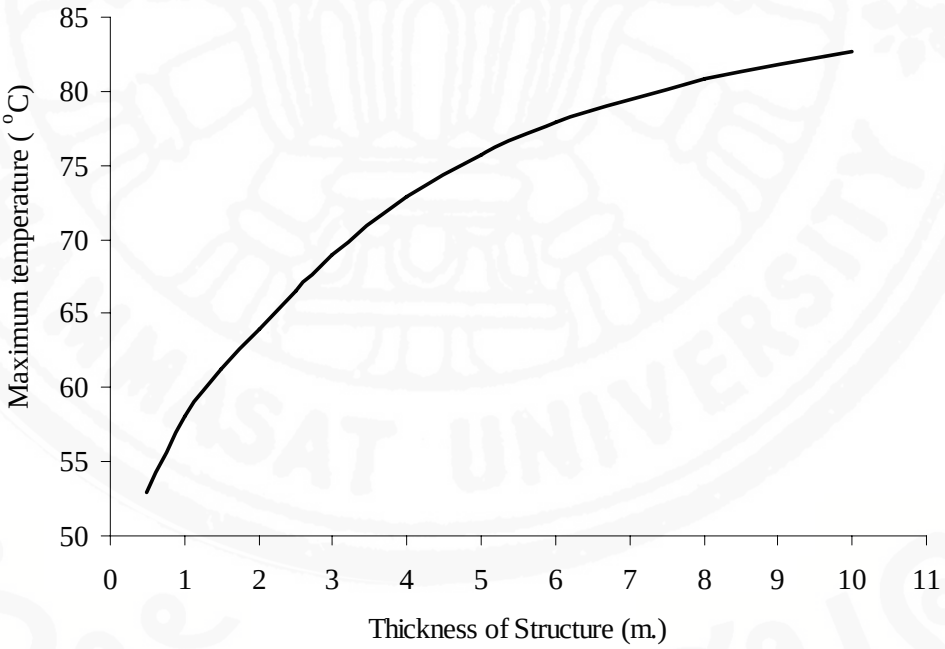

Fig. 9.9 Relationship between maximum temperature and thickness of a mass concrete

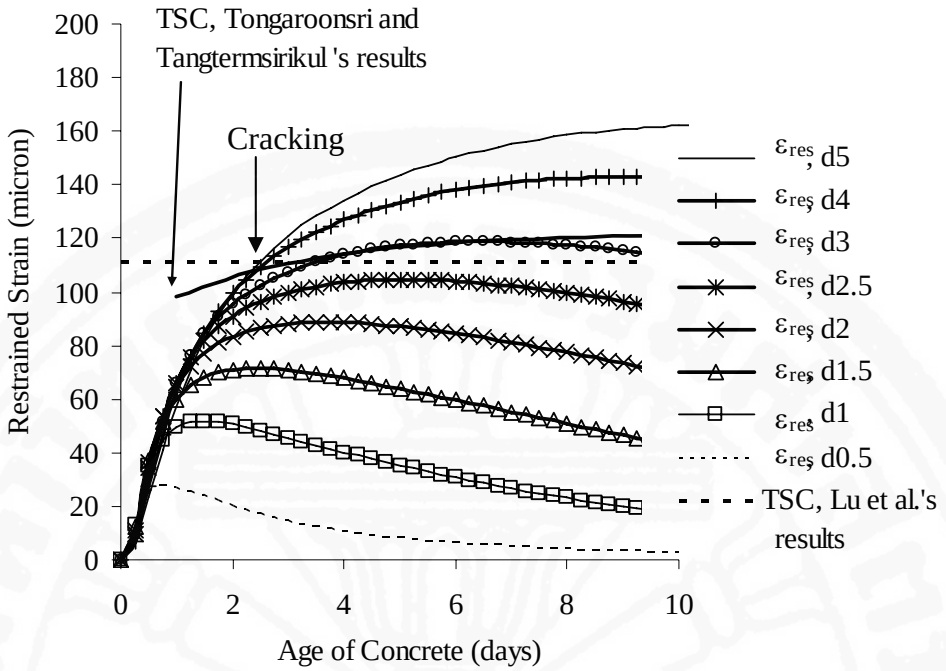

Fig. 9.10 Predicted restrained strain of mass concrete with different thickness (width = 33 m., length = 49.2 m)

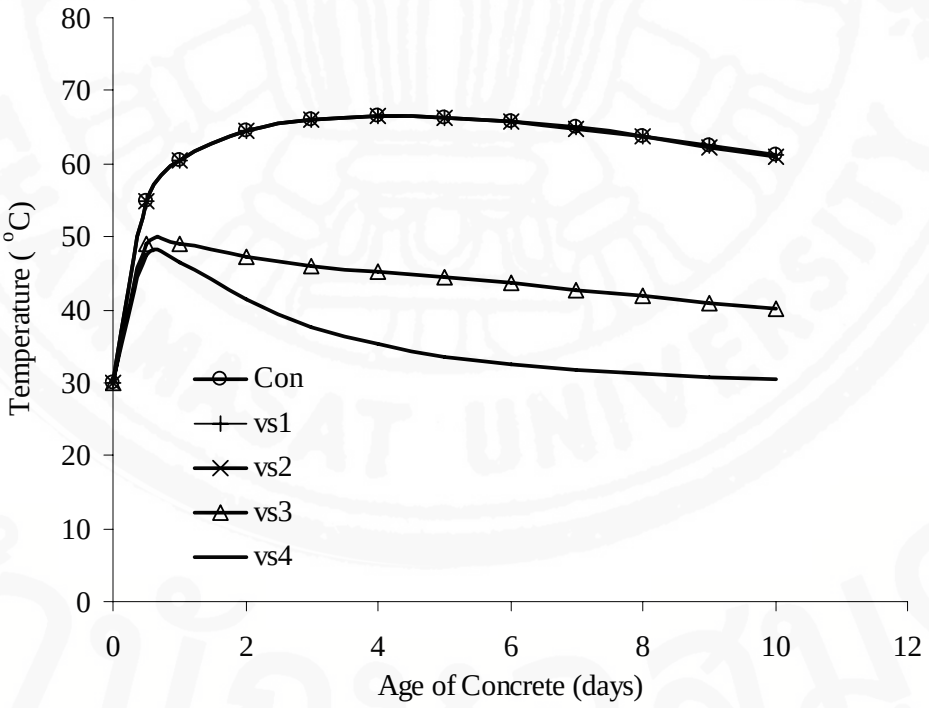

Fig. 9.11 Predicted temperature of mass concrete structure at the thickness of 2.5 m. with different width and length

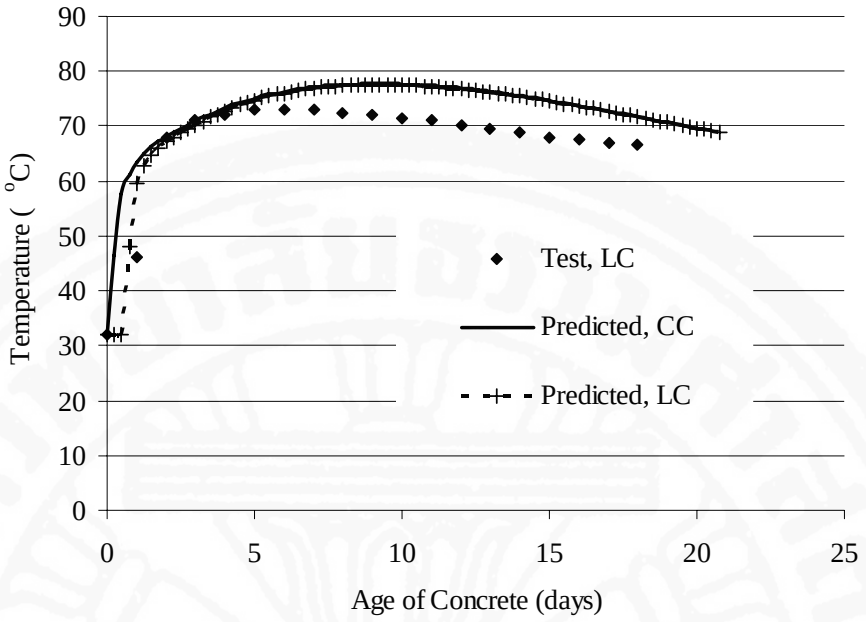

Fig. 9.12 Comparison between test and predicted temperature at center part of a mass concrete.

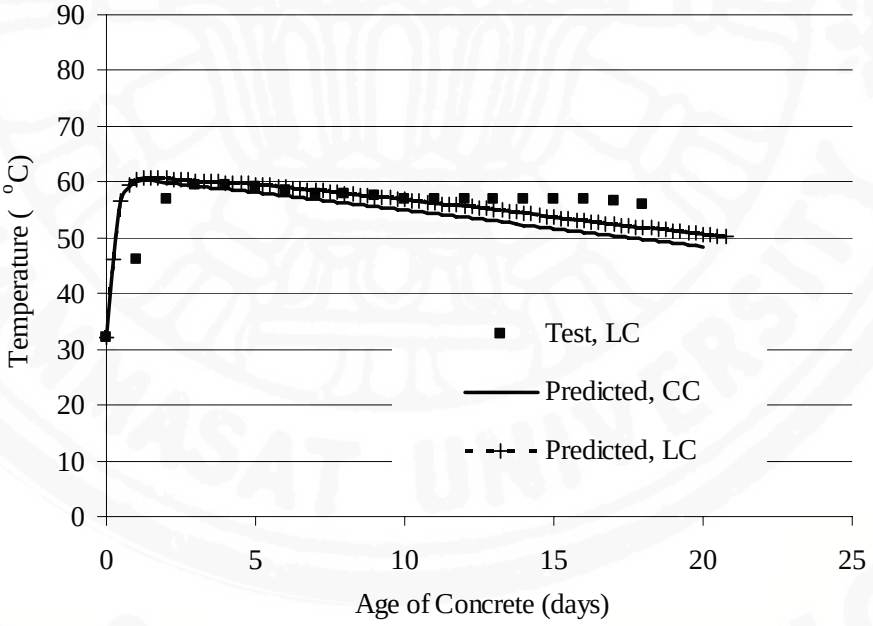

Fig. 9.13 Comparison between test and predicted temperature at bottom part of a mass concrete.

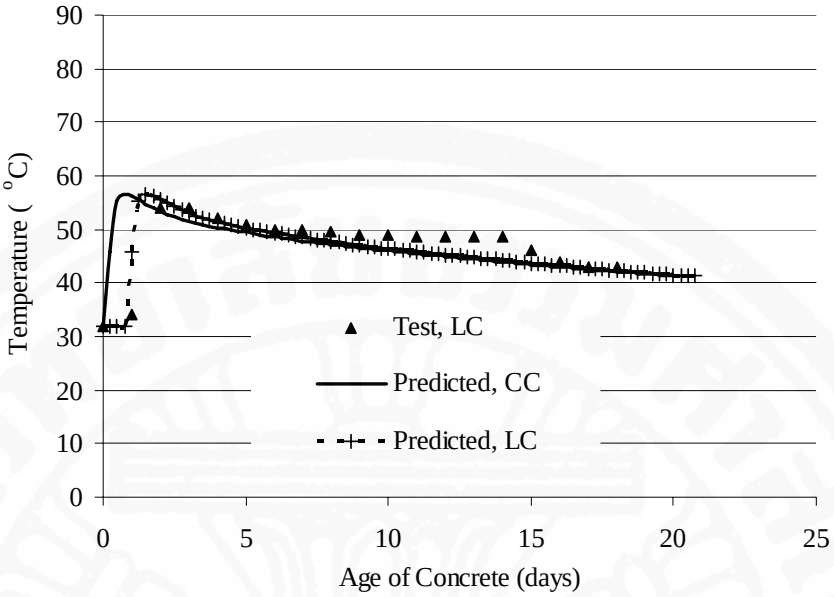

Fig. 9.14 Comparison between test and predicted temperature at top part of a mass concrete.

b) Casting method.

The analytical results in Fig. 9.10 show that the analyzed mass concrete structures with thickness higher than 3 m. tend to crack because the $\varepsilon_{res,\ ten}$ is higher than TSC. In order to prevent thermal cracking, several techniques are possible. One of them is to apply discontinuous casting method. The footing with the thickness of 3 m. was used as an example to study the effect of casting method.

It was found from the analytical results that the concrete block 1 is the most critical part then the results of concrete block 1 were used for discussion in this study. The analytical results at core zone of concrete block 1 as shown in Figs 9.15, 9.16 and 9.17 are used to describe the predicted temperature and $\varepsilon_{res,\ ten}$ at the top surface in lateral and longitudinal directions of footing (see Fig. 9.18). From Fig 9.15, it can be seen that temperature of different casting methods are nearly the same except for the case of layer casting method. Temperature of concrete is mainly dependent on the thickness (smallest dimension) rather than width and length. The thickness of continuous casting and block casting method are the same but for the layer casting the thickness was reduced by half, then the temperature gradient of layer casting method is the lowest. From this reason, $\varepsilon_{res,\ ten}$ of the layer casting method in both lateral and longitudinal direction is the lowest as shown in Figs 9.16 and 9.17. In the case of block casting method, the smaller volume of concrete block results in the smaller restrained strain in the lateral direction as shown in Fig 9.15 (comparing 4B with 2B). In the longitudinal direction, the use formwork results in the change of the boundary condition. The heat loss to surrounding on this surface is highest when compared to other surfaces. Then temperature gradient between center and side surface of block casting method is higher than continuous casting method. As a result, $\varepsilon_{res,\ ten}$ is higher when compared with the case of continuous casting method (as shown in Fig 9.16).

However, the most severe part of block casting occurred at the joint between each block as shown in Figs 9.19a and b. According to the use of steel formwork, temperature gradient between center and this surface is the highest when compared to other surfaces then the $\varepsilon_{res,\ ten}$ on this surface is the highest. When compare $\varepsilon_{res,\ ten}$ to TSC, it was found that both 2B and 4B casting have high chance to crack at top surface due to thermal cracking. Fig 9.20 shows that the severity increases after the casting of second block at the cold joint. During heating up stage of the second block, the first block is pulled by the second block resulting in rapid increase of the restrained strain on the side surface of the first block. For layer casting, the most critical point occurs at the bottom surface of the first layer (see Fig. 9.19c). During heating up stage of the second layer, the heat on the top layer transfer to the bottom layer then the temperature on the top surface of the first layer increases as shown in Fig 9.15. This results in the change of the phenomena of footing to be the same as continuous casting where the center is subjected to compressive restraint while the top and bottom surfaces are subjected to tensile restraint. The $\varepsilon_{res,\ ten}$ at the bottom face increases rapidly after the casting of the second part (as shown in Fig. 9.20). From Figs 9.16, 9.17 and 9.20, $\varepsilon_{res,\ ten}$ was compared to TSC and it was found that the layer casting is the most effective method for the control of thermal cracking. In real practice, it is recommended to provide adequate amount of temperature steel near the former cast surface of each cold joint or near the exposed surfaces of the mass concrete in order to reduce the possibility of cracking and to minimize the thermal crack width to be within the acceptable value if cracking is unavoidable. It must be mentioned here that in this analysis, the cold joints between each blocks are assumed to have perfect bond. The modulus of elasticity of concrete at early age especially at a few hours after casting is much lower than the value used in this analysis then the increasing of the restrained strain after the casting of the second block is not as fast as that shown in this paper. However, the analytical results can be used to illustrate the behavior as that occurs in the real practice of discontinuous casting of mass concrete with reasonable results.

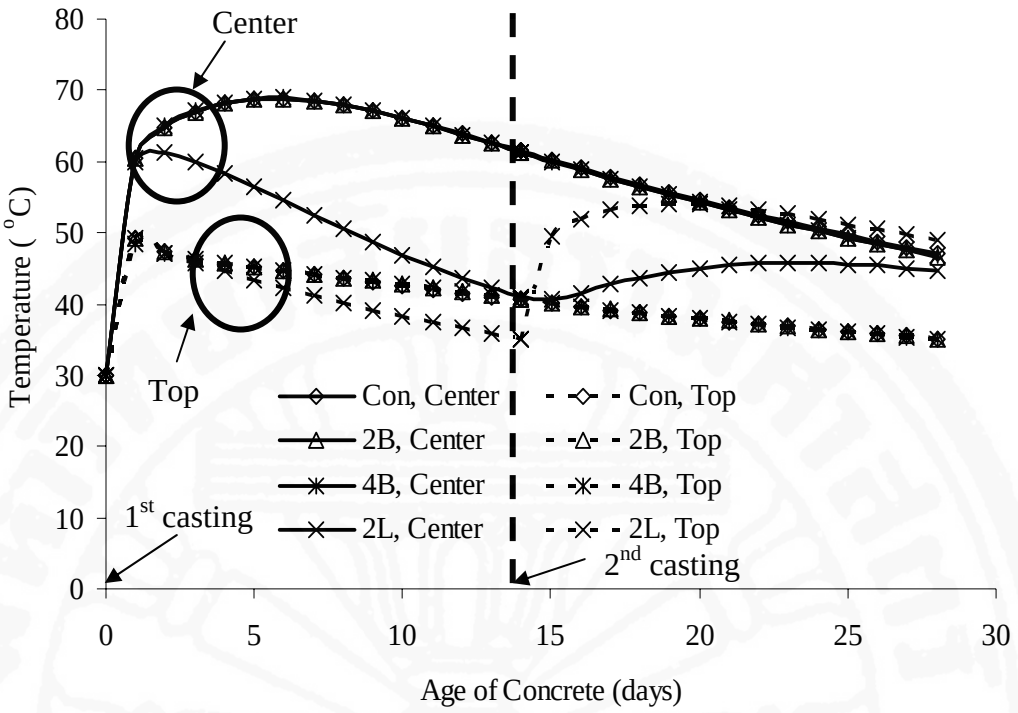

Fig. 9.15 Predicted temperature of the first part of mass concrete structure with different casting methods

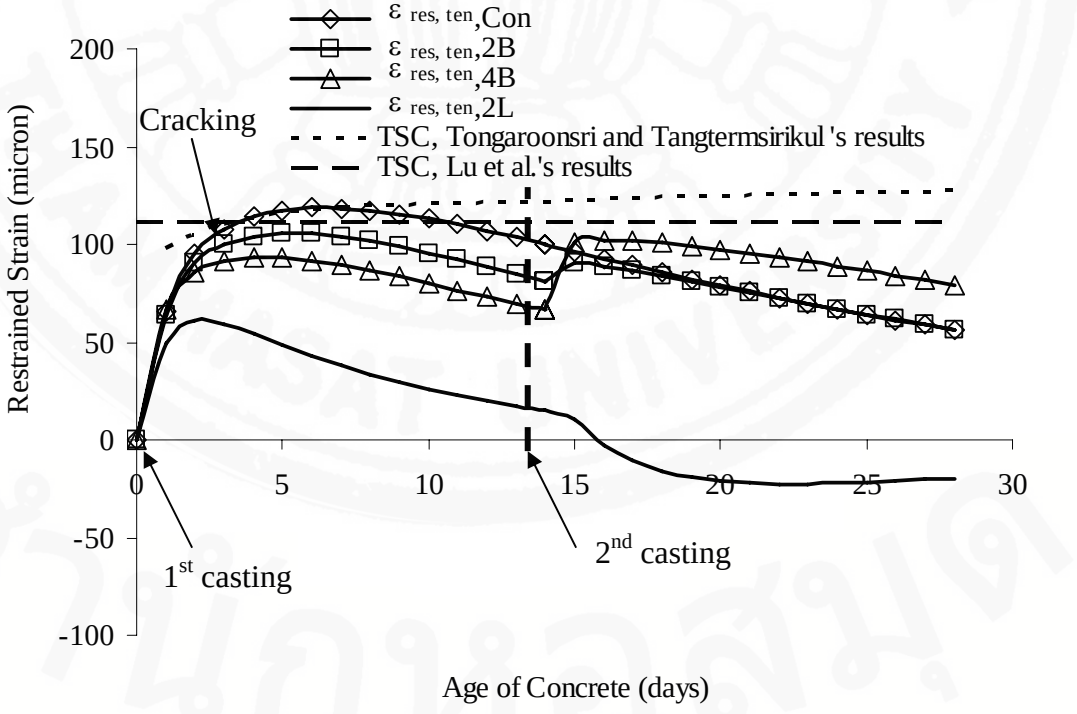

Fig. 9.16 Predicted restrained strain at the top surfaces in the lateral direction of mass concrete structure of the first casting part

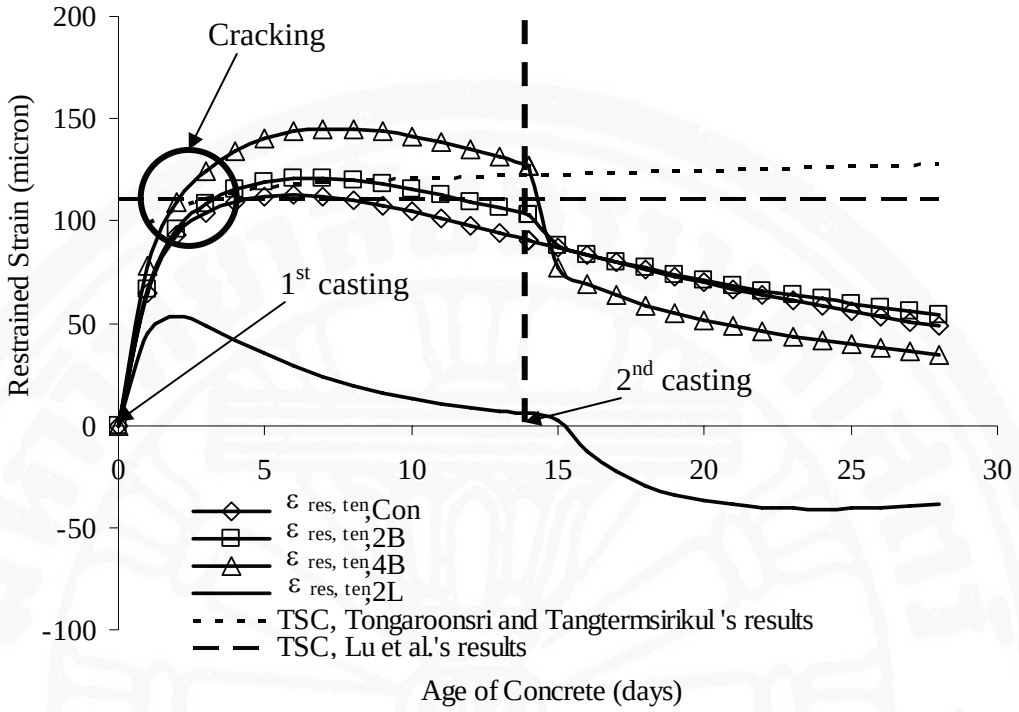

Fig. 9.17 Predicted restrained strain at the top surfaces in the longitudinal direction mass concrete structure of the first casting part

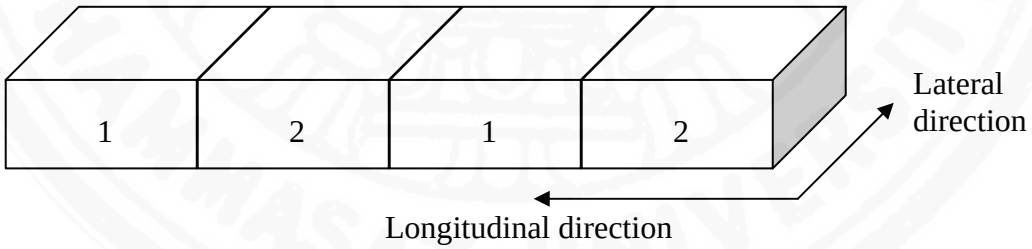

Fig. 9.18 Direction of restrained strains of a mass concrete structure (4B)

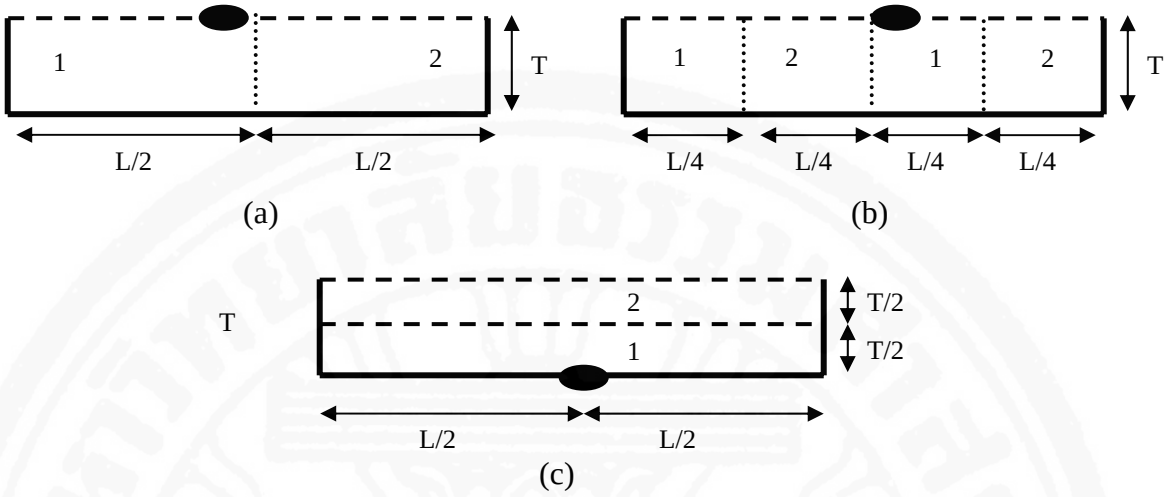

Fig. 9.19 Critical points of block and layer casting (side view). (a). Discontinuous casting with 2-block casting. (b) Discontinuous casting with 4-block casting. (c). Discontinuous casting with 2-layer casting.

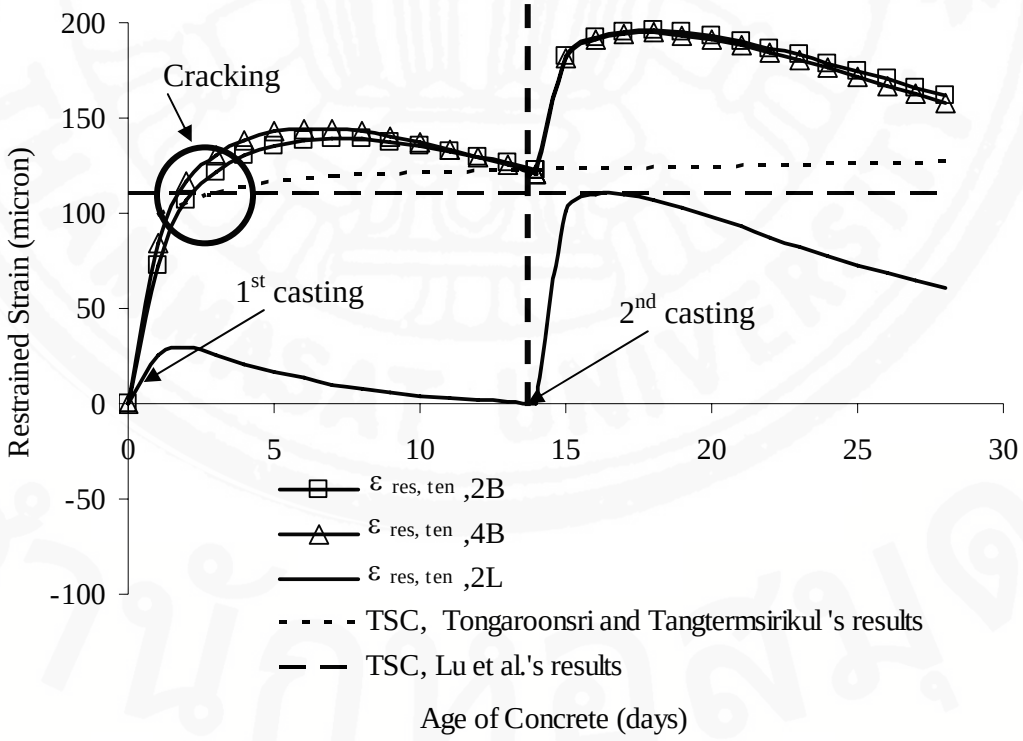

Fig. 9.20 Predicted restrained strain in the lateral direction of mass concrete structure at the critical point.

c) Curing condition and curing period.

As shown in Fig 9.10, footing with thickness 2.5 m. is safe from thermal cracking when CIC curing method is used. However, the use of inappropriate curing condition and curing period increases crack risk of the footing. Fig 9.21 shows the temperature at center and top surfaces of concrete with different curing methods. The temperature differences between center and top surfaces of the structure cured by NC method is higher than CIC method and then causes higher $\varepsilon_{res,\ ten}$ (as shown in Fig 9.22). $\varepsilon_{res,\ ten}$ of NC is higher than TSC then the use of NC results in the higher risk of cracking when compared to CIC. The application of insulation curing is recommended for mass concrete.

Figs 9.23 and 9.24 show the temperature and $\varepsilon_{res,\ ten}$ of concrete footing cured by insulation curing method with varied insulation curing periods. It is shown that if the insulation material is too early removed (at 7 days), the surface temperature reduces rapidly. As a result, temperature difference between center and top surfaces increases rapidly and thermal cracking may occur. The $\varepsilon_{res,\ ten}$ is higher than TSC when the insulation material is too early removed then it causes crack after the removal of the insulation material. Fig 9.24 shows that the longer insulation curing period (14 days) results in lower $\varepsilon_{res,\ ten}$ or in other word the severity becomes smaller when the insulation curing period is longer. As a result, $\varepsilon_{res,\ ten}$ of the longer curing period is always lower than TSC. It is then recommended that temperature monitoring should be done to prevent the premature removal of the insulation material. The center-ambient temperature difference and the surface-ambient temperature difference at the removal of insulation material should be controlled properly. The insulation curing period should be continued long enough.

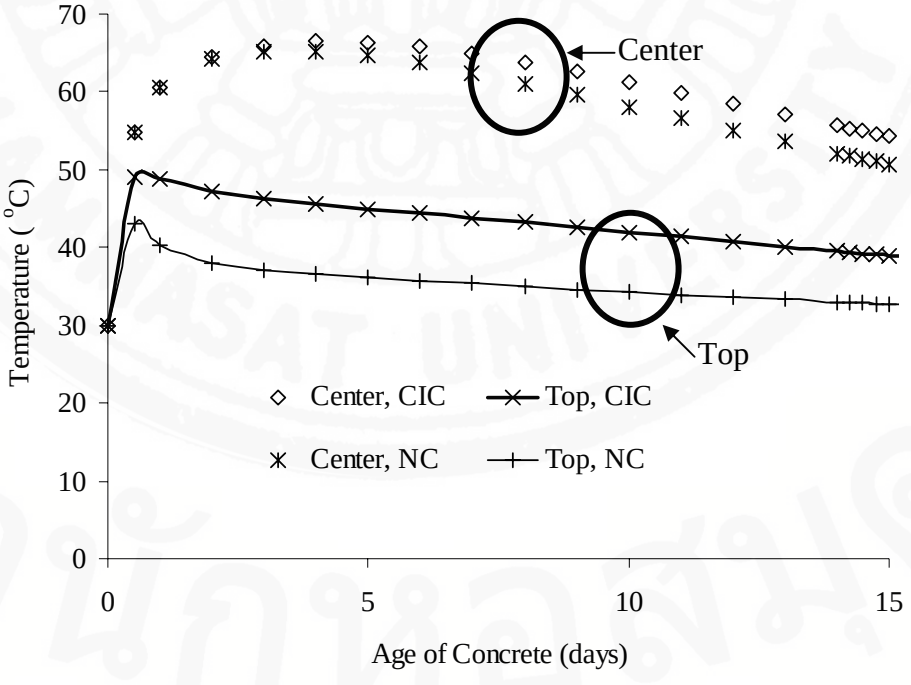

Fig. 9.21 Predicted temperature of a mass concrete cured by normal and insulated curing methods

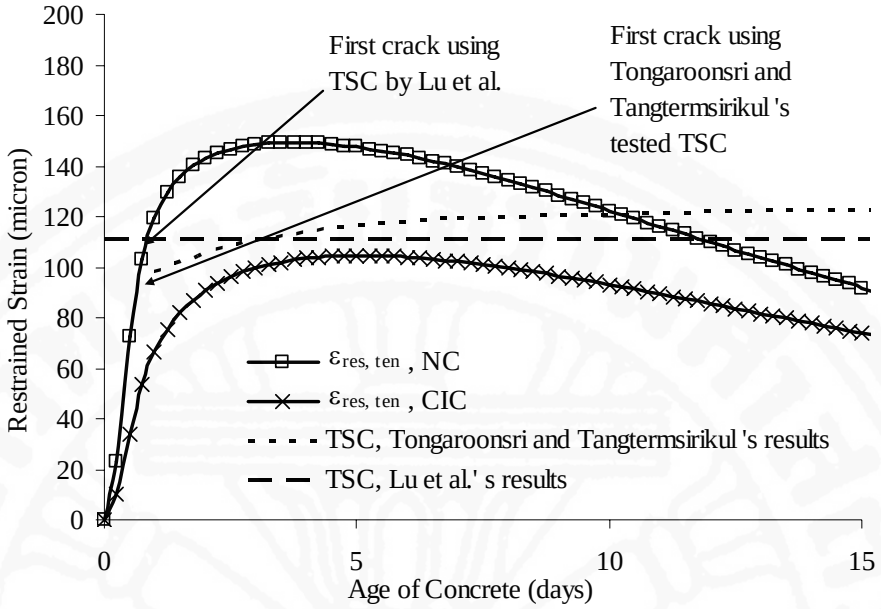

Fig. 9.22 Predicted restrained strain of a mass concrete cured by normal and insulated curing methods

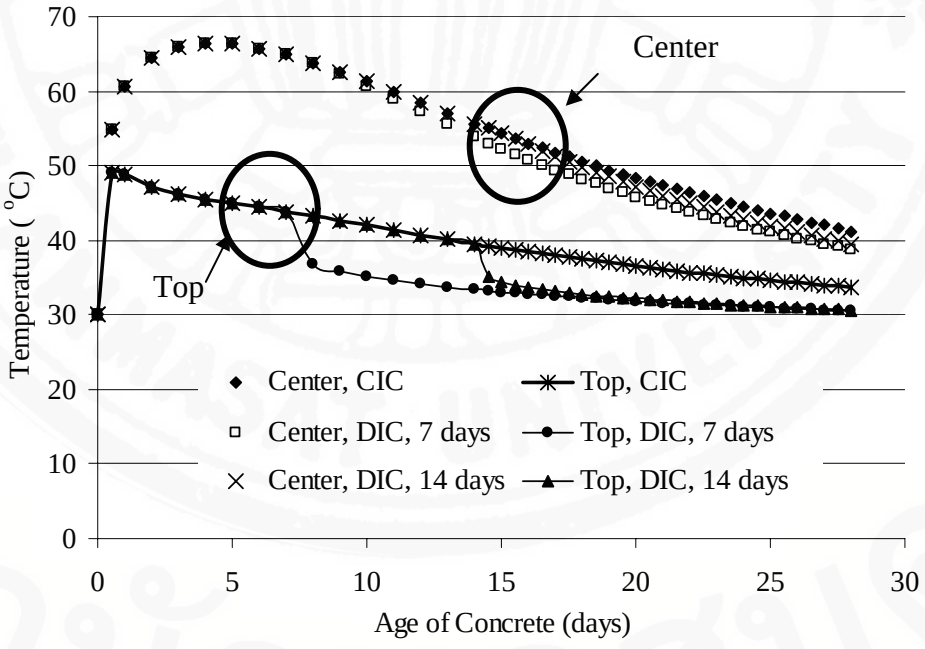

Fig. 9.23 Predicted temperature of a mass concrete cured by continuous and discontinuous insulated curing methods

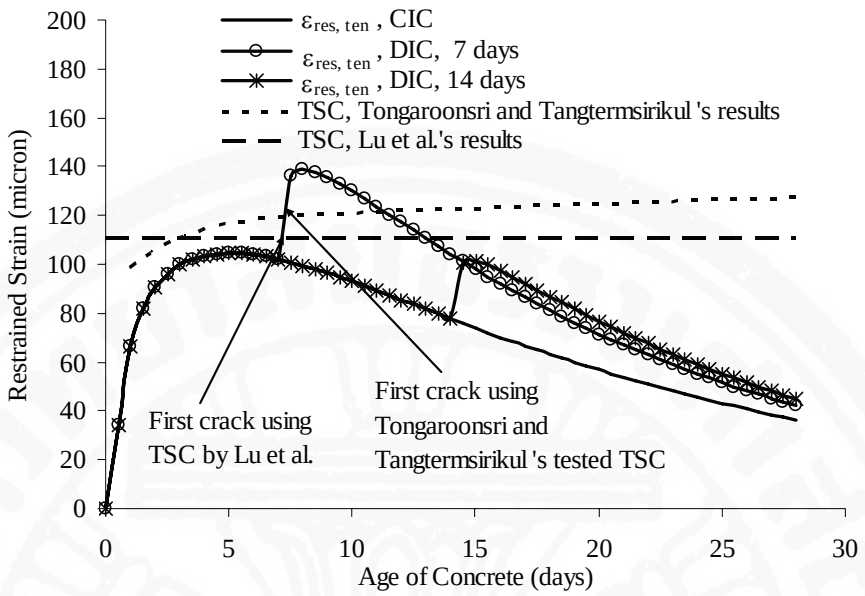

Fig. 9.24 Predicted restrained strain of mass concrete structure with different insulated curing periods